

Theoretical Analysis of the Unusual Vicinal Effects on Electronic Circular Dichroism Spectra of Cobalt(III) Complexes with ED3A-Type and Related Ligands

Yuekui Wang and Chunxia Zhang

Key Laboratory of Chemical Biology and Molecular Engineering of the Education Ministry, Institute of Molecular Science, Shanxi University, Taiyuan, Shanxi 030006, P. R. China

Reprint requests to Y. W.; E-mail: ykwang@sxu.edu.cn

Z. Naturforsch. **69a**, 371–384 (2014) / DOI: 10.5560/ZNA.2014-0032

Received March 10, 2014 / April 4, 2014 / published online July 15, 2014

This article is dedicated to Professor Jörg Fleischhauer on the occasion of his 75th birthday.

To investigate the origin of unusual *N*-vicinal effects, the geometries of the two series of cobalt(III) complexes, $[\text{Co}(\text{ED3A-type})(X)]^-$ ($X = \text{CN}^-$, NO_2^-) and $[\text{Co}(\text{EDDS-type})]^-$, with the pentadentate ethylenediamine-*N,N,N'*-triacetate (ED3A), hexadentate (*S,S*)-ethylenediamine-*N,N'*-dissuccinate (EDDS), and their *N*-alkyl-substituted ligands in aqueous solution have been optimized at the DFT/B3P86/6-311++G(2d,p) level of theory. Based on the optimized geometries, the excitation energies and rotational strengths have been calculated using the time dependent density functional theory (TDDFT) method with the same functional and basis set. The optimized geometries and calculated electronic circular dichroism (ECD) curves are in good agreement with the observed ones. Based on this agreement, the characteristics of usual and unusual *N*-vicinal effects as well as the related chiral stereochemistry phenomena have been discussed. To reveal the origin of the unusual *N*-vicinal effects, a novel calculation scheme has been proposed, which permits efficiently assessing the contribution of the octahedral core to the optical activities of the chelates. The results show that the substituent effects and conformational relaxation effects make opposite contributions to the overall *N*-vicinal effects with the former being dominant. The unusual *N*-vicinal effects originate from the negligible chirality of the octahedral core in the unsubstituted $[\text{Co}(\text{ED3A})(X)]^-$ chelates. For this reason, their optical activity is dominated by the asymmetric nitrogens and behaves different from the normal cases. The unusual vicinal effects observed in the *N*-alkyl-substituted ED3A-type chelates reflect an increase in the contribution of the octahedral core to their optical activity, which recovers the ECD spectra from the special cases to the normal ones.

These findings provide some insight into the unusual *N*-vicinal effects as well as the chiroptical properties of the chelates.

Key words: Co(III)-ED3A Chelates; Co(III)-EDDS Chelates; ECD Spectra; TDDFT Calculations.

1. Introduction

The investigation of chiroptical properties of transition metal complexes has received much attention over the past century, with considerable efforts focused on the correlation between experimental parameters of electronic circular dichroism (ECD) and specific stereochemical features of the metal chelates. In this field, much work has been done both experimentally [1, 2] and theoretically [3, 4]. Many theoretical models [5, 6] and empirical or semi-empirical rules [7, 8] have been established. Each of them has enjoyed some success in explaining or rationalizing the observed spectra. However, there remain some interesting experimental

phenomena which are not yet well understood. The reason for this is partly due to the fact that transitions in metal complexes are more complex than in organic molecules, partly may be attributed to a lack of extensive theoretical analyses, especially at the first-principle level.

For example, it is known that rotational strengths of transition metal complexes in the *d-d* absorption region are not only governed by the distribution of chelate rings about the central metal ion (configurational effect, e. g., the Δ/Λ octahedral core) and the conformations of the chelate rings (conformational effect, e. g., the δ/λ twists of chelate rings), but also by the vicinal effects of some asymmetric

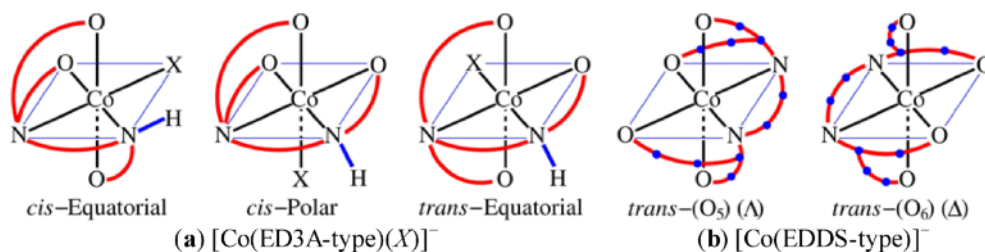


Fig. 1 (colour online). Possible geometric isomers of six-coordinate complexes: (a) with a pentadentate ED3A-type ligand, (b) with a hexadentate (*S,S*)-EDDS-type ligand.

donor atoms, as indicated by Maricondi and Douglas [9] in 1972. In their study on the ECD spectra of *s-cis*- $[\text{Co}(\text{EDDA-type})(L)]^\pm$ complexes with the tetradentate ligands ethylenediamine-*N,N'*-diacetate (EDDA), *N,N'*-dimethyl-EDDA (DMEDDA), *N,N'*-diethyl-EDDA (DEEDDA), as well as a bidentate ancillary ligand *L* (*L* = ethylenediamine, oxalate), they found that the ECD peak intensities of all the *N*-alkyl-substituted complexes are less than half those of the corresponding unsubstituted EDDA complexes. This reduction in intensities was thought to be reasonable because all the groups about the nitrogen are similar, differing only in the second or third atom from the nitrogen. In other words, the asymmetry of alkyl-substituted nitrogens is less than that of unsubstituted ones. Therefore, this effect is called vicinal effect. In this sense, it seems impossible to reverse the sign of rotational strengths or ECD spectra only by the vicinal effects. However, just one year later, Maricondi and Maricondi [10] found that the isomers of $[\text{Co}(\text{ED3A})(\text{NO}_2)]^-$ and $[\text{Co}(\text{BED3A})(\text{NO}_2)]^-$ (ED3A is the pentadentate

ethylenediamine-*N,N,N'*-triacetate anion, BED3A is the corresponding *N*-benzyl-substituted ligand) with comparable structures give ECD curves which have opposite signs over most of the *d-d* absorption region; i. e., the substituted asymmetric nitrogen donor atoms make opposite contributions to the rotational strengths of the complexes when compared with the unsubstituted counterpart. The same phenomenon was also observed by Radanovic et al. [11] in the *cis-eq*- $[\text{Co}(\text{ED3A-type})(\text{CN})]^-$ complexes. Even in the $[\text{Co}(\text{EDDS-type})]^-$ complexes (EDDS is the hexadentate (*S,S*)-ethylenediamine-*N,N'*-disuccinate anion), which are structurally similar to the $[\text{Co}(\text{EDDA})(\text{ox})]^-$ series, only negligible *N*-vicinal effects were observed by Jordan and Legg [12] in 1974. These results raise questions on the nature of the *N*-vicinal effects.

There has been some effort to elucidate the unusual *N*-vicinal effects according to the theoretical models [13, 14] and regional rules [8, 15], but these formal theories may not be adequate for this purpose. In recent decades, however, with the development of density functional theory (DFT) and especially the im-

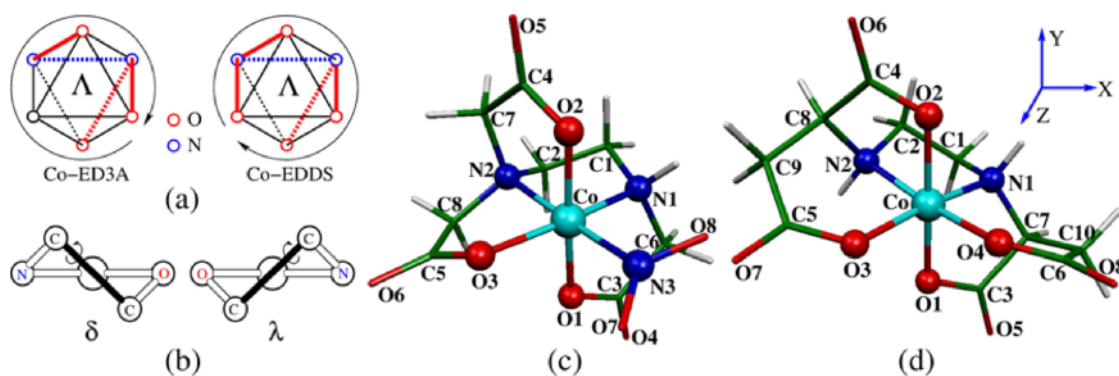


Fig. 2 (colour online). (a) Λ -octahedral cores of Co-ED3A and Co-EDDS complexes; (b) δ/λ twists of five-membered chelate rings; (c) absolute configuration of *cis-eq*- $\text{C}_1\Lambda(R)(\delta)(\lambda\lambda\lambda)[\text{Co}(\text{ED3A})(\text{NO}_2)]^-$ complex; (d) absolute configuration of *trans*-(O_5)- $\text{C}_2\Lambda(\text{SS},\text{RR})(\lambda)(\delta'\delta')_e(\lambda\lambda)_a[\text{Co}(\text{EDDS})]^-$ chelate.

Table 1. Comparison of the calculated and observed structural parameters[†] of the isomers *cis-eq*-C₁A(R)(δ)($\lambda\lambda\lambda$)[Co(ED3A)(NO₂)]⁻ and *trans*-(O₅)-C₂A(SS,RR)(λ)($\delta'\delta'$)_e($\lambda\lambda$)_a[Co(EDDS)]⁻.

<i>cis-eq</i> -C ₁ A(R)(δ)($\lambda\lambda\lambda$)[Co(ED3A)(NO ₂)] ⁻						<i>trans</i> -(O ₅)-C ₂ A(SS,RR)(λ)($\delta'\delta'$) _e ($\lambda\lambda$) _a [Co(EDDS)] ⁻					
Lengths	Calc.	X-ray [22]	Angles	Calc.	X-ray [22]	Lengths	Calc.	X-Ray [25]	Angles	Calc.	X-ray [25]
Co–N1	1.952	1.954	N1–Co–N2	88.4	87.7	Co–N1	1.952	1.904	N1–Co–N2	87.6	87.7
Co–N2	1.969	1.964	N1–Co–O1	85.3	86.3	Co–O1	1.919	1.889	N1–Co–O1	82.8	84.0
Co–N3	1.917	1.922	N2–Co–O2	87.3	87.3	Co–O3	1.927	1.922	N1–Co–O4	93.0	93.5
Co–O1	1.899	1.882	N2–Co–O3	83.5	83.2	C1–C2	1.514	1.519	N1–Co–O2	95.2	96.1
Co–O2	1.885	1.884	N3–Co–O1	91.0	90.2	N1–C1	1.494	1.494	O2–Co–O3	92.0	91.9
Co–O3	1.906	1.919	N3–Co–O2	88.9	88.7	N1–C7	1.486	1.491	O2–Co–O4	90.0	88.0
C1–C2	1.514	1.514	N3–Co–O3	95.7	94.1	C3–O1	1.295	1.295	N1–C1–C2–N2	–47.8	–49.9
N3–O7	1.222	1.230	N1–C1–C2–N2	52.3	54.0	C3–O5	1.226	1.230	N2–C8–C4–O2	–24.2	–20.9
N3–O8	1.235	1.229	N1–Co–N3–O8	28.0	–33.4	C3–C7	1.539	1.529	N2–C8–C9–C5	57.1	57.3

[†] Bond lengths are in Ångströms, bond angles and dihedral angles in degrees. The corresponding observed value is the mean value of symmetry equivalents. Atom numbering refers to Figures 2c and d.

provement of time dependent density functional theory (TDDFT) [16], properties of both ground- and excited-states for medium-sized metal complexes can be calculated at the first-principle level with good accuracy [17, 18]. This makes it possible to perform such an analysis for these chelates.

It is generally agreed that the vicinal effects of asymmetric nitrogens involve not only a change in substituents, but also in the conformations of related chelates. To clarify the nature of *N*-vicinal effects it is necessary to make it clear which change dominates the effects. Previously [18], we have reported a theoretical analysis of the cobalt(III) EDDA-type complexes, and found that the two changes make synergistic con-

tributions to the *N*-vicinal effects, but the change in substituents is dominant.

In this paper, we shall present and discuss calculations of the two series of cobalt(III) chelates [Co(ED3A-type)(X)]⁻ ($X = \text{CN}^-$, NO_2^-) and [Co(EDDS-type)]⁻ at the first-principial level. The main object of this research is to clarify the nature of the unusual *N*-vicinal effects found in these systems and to elucidate the relationship between chiroptical properties and stereochemical features of the chelates. The computational details are summarized in the next section. Analyses and discussions on the results are presented in the section thereafter. Finally, the main conclusions and findings are given in the last section.

Table 2. Symmetries of excited states (Sym), excitation wavelengths (λ), oscillator (f) and rotational (R) strengths, electric (μ) and magnetic (m) dipole transition moments as well as the angle (θ) between them for the first 6 transitions of the *cis-eq*-[Co(ED3A-type)(CN)]⁻ chelates.

Sym	λ (nm)	f	R (DBM)	$ \mu $ (D)	$ m $ (BM)	θ (deg)	Assignments [†]
C ₁ A(R)(δ)($\lambda\lambda\lambda$)[Co(ED3A)(CN)] ⁻							
2 ¹ A	560.48	0.0008	–0.0240	0.3025	1.7305	93.0	$dyz(p\pi) + n_O \rightarrow \sigma_{\text{CoO,CoN}}^*(dx^2-y^2)$
3 ¹ A	475.83	0.0003	0.0047	0.1821	1.6382	90.0	$dxy(p\sigma) + n_O \rightarrow \sigma_{\text{CoO,CoCN}}^*(dxz)$
4 ¹ A	450.83	0.0013	0.0497	0.3546	1.5647	84.5	$dz^2(p\pi) + n_O \rightarrow \sigma_{\text{CoO,CoN}}^*(dx^2-y^2)$
5 ¹ A	380.30	0.0004	0.0114	0.1806	0.2361	73.0	$dxy(p\sigma) + n_O \rightarrow \sigma_{\text{CoO,CoN}}^*(dx^2-y^2)$
6 ¹ A	368.51	0.0012	0.0352	0.3025	0.2020	54.7	$dyz(p\pi) + n_O \rightarrow \sigma_{\text{CoO,CoCN}}^*(dxz)$
7 ¹ A	353.37	0.0012	–0.0207	0.3045	0.2341	107.0	$dz^2(p\pi) + n_O \rightarrow \sigma_{\text{CoO,CoCN}}^*(dxz)$
C ₁ A(R)(δ)($\lambda\lambda\lambda$)[Co(MED3A)(CN)] ⁻							
2 ¹ A	565.38	0.0007	0.0149	0.2861	1.7418	88.2	$dyz(p\pi) + n_O \rightarrow \sigma_{\text{CoO,CoCN}}^*(dxz)$
3 ¹ A	475.85	0.0002	–0.0052	0.1591	1.6365	89.8	$dxy(p\sigma) + n_O \rightarrow \sigma_{\text{CoO,CoN}}^*(dx^2-y^2)$
4 ¹ A	459.61	0.0013	–0.0059	0.3630	1.5826	90.5	$dz^2(p\pi) + n_O \rightarrow \sigma_{\text{CoO,CoCN}}^*(dxz)$
5 ¹ A	386.34	0.0005	0.0213	0.1954	0.2570	63.9	$dxy(p\sigma) + n_O \rightarrow \sigma_{\text{CoO,CoCN}}^*(dxz)$
6 ¹ A	370.64	0.0010	0.0267	0.2778	0.1741	57.0	$dyz(p\pi) + n_O \rightarrow \sigma_{\text{CoO,CoN}}^*(dx^2-y^2)$
7 ¹ A	352.61	0.0012	–0.0168	0.2980	0.2389	103.6	$dz^2(p\pi) + n_O \rightarrow \sigma_{\text{CoO,CoN}}^*(dx^2-y^2)$

[†] $dxy(p\sigma) = dxy + \sigma_{\text{CoCN}}$, $dz^2(p\pi) = dz^2 + \pi_{\text{COO}} + \pi_{\text{CN}}$, and $dyz(p\pi) = dyz + \pi_{\text{COO}}$ with some $d-p\pi$ conjugation; n_O is always mixed with the σ_{CCO} orbital of the carboxyl groups.

Table 3. Symmetries of excited states (Sym), excitation wavelengths (λ), oscillator (f) and rotational (R) strengths, electric (μ) and magnetic (m) dipole transition moments as well as the angle (θ) between them for the first 6 transitions of the *cis-eq*-[Co(ED3A-type)(NO₂)]⁻ chelates.

Sym	λ (nm)	f	R (DBM)	$ \mu $ (D)	$ m $ (BM)	θ (deg)	Assignments [†]
$C_1\Lambda(R)(\delta)(\lambda\lambda\lambda)[\text{Co}(\text{ED3A})(\text{NO}_2)]^-$							
2 ¹ A	553.69	0.0008	-0.0202	0.2975	1.7168	92.2	$dyz(p\pi) + n_{\text{O}} \rightarrow \sigma_{\text{CoO,CoN}}^*(dxz)$
3 ¹ A	482.29	0.0006	-0.0423	0.2534	1.7427	95.4	$dxy(p\pi) + n_{\text{O}} \rightarrow \sigma_{\text{CoO,CoN}}^*(dx^2-y^2)$
4 ¹ A	461.53	0.0012	0.0772	0.3486	1.7105	82.6	$dz^2(p\sigma) + n_{\text{NO}_2} \rightarrow \sigma_{\text{CoO,CoN}}^*(dxz)$
5 ¹ A	386.11	0.0005	0.0059	0.2028	0.0710	65.7	$dyz(p\pi) + n_{\text{O}} \rightarrow \sigma_{\text{CoO,CoN}}^*(dx^2-y^2)$
6 ¹ A	375.57	0.0011	0.0221	0.2902	0.2155	68.0	$dxy(p\pi) + n_{\text{O}} \rightarrow \sigma_{\text{CoO,CoN}}^*(dxz)$
7 ¹ A	355.98	0.0019	-0.0132	0.3764	0.1943	101.0	$dz^2(p\sigma) + n_{\text{NO}_2} \rightarrow \sigma_{\text{CoO,CoN}}^*(dx^2-y^2)$
$C_1\Lambda(R)(\delta)(\lambda\lambda\lambda)[\text{Co}(\text{MED3A})(\text{NO}_2)]^-$							
2 ¹ A	565.46	0.0008	0.0355	0.3131	1.7296	86.4	$dxy(p\pi) + n_{\text{O}} \rightarrow \sigma_{\text{CoO,CoN}}^*(dxz)$
3 ¹ A	485.93	0.0003	0.0027	0.1735	1.7361	90.0	$dyz(p\pi) + n_{\text{O}} \rightarrow \sigma_{\text{CoO,CoN}}^*(dx^2-y^2)$
4 ¹ A	472.85	0.0011	-0.0380	0.3320	1.7215	93.4	$dz^2(p\sigma) + n_{\text{NO}_2} \rightarrow \sigma_{\text{CoO,CoN}}^*(dxz)$
5 ¹ A	392.73	0.0001	0.0069	0.1012	0.2096	70.8	$dyz(p\pi) + n_{\text{O}} \rightarrow \sigma_{\text{CoO,CoN}}^*(dxz)$
6 ¹ A	384.55	0.0016	0.0399	0.3659	0.2045	58.0	$dxy(p\pi) + n_{\text{O}} \rightarrow \sigma_{\text{CoO,CoN}}^*(dx^2-y^2)$
7 ¹ A	353.45	0.0015	-0.0315	0.3363	0.2373	112.3	$dz^2(p\sigma) + n_{\text{NO}_2} \rightarrow \sigma_{\text{CoO,CoN}}^*(dx^2-y^2)$
$C_1\Lambda(R)(\delta)(\lambda\lambda\lambda)[\text{Co}(\text{BED3A})(\text{NO}_2)]^-$							
2 ¹ A	571.48	0.0011	0.0479	0.3682	1.7149	85.7	$dxy + \pi_{\text{B}} + n_{\text{O}} \rightarrow \sigma_{\text{CoO,CoN}}^*(dxz)$
3 ¹ A	484.88	0.0003	-0.0557	0.1732	1.7370	100.8	$dyz + n_{\text{O}} + \sigma_{\text{CoNO}_2} \rightarrow \sigma_{\text{CoO,CoN}}^*(dx^2-y^2)$
4 ¹ A	477.06	0.0018	-0.0123	0.4304	1.7114	90.6	$dz^2(p\sigma) + n_{\text{NO}_2} \rightarrow \sigma_{\text{CoO,CoN}}^*(dxz)$
5 ¹ A	396.04	0.0002	0.0243	0.1380	0.2396	44.2	$dyz + n_{\text{O}} + \sigma_{\text{CoNO}_2} \rightarrow \sigma_{\text{CoO,CoN}}^*(dxz)$
6 ¹ A	385.54	0.0018	0.0262	0.3789	0.1752	66.5	$dxy + \pi_{\text{B}} + n_{\text{O}} \rightarrow \sigma_{\text{CoO,CoN}}^*(dx^2-y^2)$
7 ¹ A	353.29	0.0022	-0.0386	0.4044	0.2875	108.4	$dz^2(p\sigma) + n_{\text{NO}_2} \rightarrow \sigma_{\text{CoO,CoN}}^*(dx^2-y^2)$

[†] $dz^2(p\sigma) = dz^2 + \sigma_{\text{CoNO}_2}$; $dxy(p\pi) = dxy + \pi_{\text{COO}}$ with some $d-p\pi$ conjugation; n_{NO_2} are the lone-pair electrons on the nitro oxygens; π_{B} is the π orbital of the benzyl group. See footnotes of Table 2 for other information.

2. Computational Details

In the mixed-ligand cobalt(III) complexes [Co(ED3A-type)(X)]⁻ ($X = \text{CN}^-$, NO_2^-), the flexible pentadentate ED3A-type ligand can occupy five of the octahedral sites around the metal ion to form three octahedral geometric isomers [19]: *cis*-equatorial, *cis*-polar, and *trans*-equatorial, as indicated in Figure 1a. In which, the *cis*-equatorial configuration are generally thought to be the most favored one. In this isomer, the complex possesses four five-membered chelate rings around the central metal ion, including three glycinate rings (*G*-rings) and one ethylenediamine ring (*E*-ring), but its octahedral core has no net chirality according to the IUPAC skew line rules [20] or ring-pairing method [21], though Bell and Blackmer [22] asserted that it ‘can be described using the proposed IUPAC nomenclature as Δ ’. This does not mean it has no chirality. In fact, by inspecting the distribution of the chelate rings around the pseudo- C_3 -symmetry axis, we see that two of them form a left-handed screw or left helix as indicated by the heavy red (heavy

gray) lines in Figure 2a, while the other two make no contribution. Therefore, the net chirality of the octahedral core should be Λ . This is agreement with the suggestion of Radanovic et al. [11], and will be used in following discussions. However, in the single ligand chelates [Co(EDDS-type)]⁻ the hexadentate (*S,S*)-EDDS-type ligand can only form two isomers theoretically, i.e., the *trans*-(O_5) and *trans*-(O_6) forms, as displayed in Figure 1b, where O_5 and O_6 represent the chelate rings in *trans* positions, being the five-membered *G*-rings and the six-membered β -alaninate rings (*B*-rings), respectively. Thus, the two isomers have opposite absolute configurations at the octahedral core; one of them is shown in Figure 2a. Besides, the five- and six-membered chelate rings can also make their contribution to the conformational chirality of the chelate by their (δ/λ) twist forms, though it is small for the two out-of-plane *G*-rings because they are nearly planer. It should be noted that the (δ/λ) twist form of the six-membered *B*-ring can also be determined according to Figure 2b due to the planar carboxyl group which makes the twist

Table 4. Symmetries of excited states (Sym), excitation wavelengths (λ), oscillator (f) and rotational (R) strengths, electric (μ) and magnetic (m) dipole transition moments as well as the angle (θ) between them for the first 6 transitions of the *trans*-(O₅)-[Co(EDDS-type)]⁻ chelates.

Sym	λ (nm)	f	R (DBM)	$ \mu $ (D)	$ m $ (BM)	θ (deg)	Assignments [†]
$C_{2v}(SS,RR)(\lambda)(\delta'\delta')_e(\lambda\lambda)_a[\text{Co(EDDS)}]^-$							
1 ¹ B	575.39	0.0006	0.0949	0.2764	1.6865	77.5	$dyz(p\sigma) + n_O \rightarrow \sigma_{\text{CoO,CoN}}^*(dx^2-y^2)$
2 ¹ A	555.88	0.0001	-0.1299	0.0796	1.7978	180.0	$dxy(p\pi) + n_O \rightarrow \sigma_{\text{CoO,CoN}}^*(dx^2-y^2)$
2 ¹ B	516.47	0.0045	0.0332	0.7025	1.7584	88.3	$dz^2(p\sigma) + n_O \rightarrow \sigma_{\text{CoO,CoN}}^*(dxz)$
3 ¹ A	406.61	0.0002	-0.0008	0.1207	0.0061	180.0	$dyz(p\sigma) + n_O \rightarrow \sigma_{\text{CoO,CoN}}^*(dxz)$
3 ¹ B	389.70	0.0003	-0.0244	0.1659	0.2029	132.9	$dxy(p\pi) + n_O \rightarrow \sigma_{\text{CoO,CoN}}^*(dxz)$
4 ¹ A	380.08	0.0013	0.0674	0.3233	0.2017	0.0	$dz^2(p\sigma) + n_O \rightarrow \sigma_{\text{CoO,CoN}}^*(dx^2-y^2)$
$C_{1v}(SS,RR)(\lambda)(\delta'\delta')_e(\lambda\lambda)_a[\text{Co(MEDDS)}]^-$							
2 ¹ A	577.14	0.0007	0.0917	0.2834	1.6993	78.5	$dyz(p\sigma) + n_O \rightarrow \sigma_{\text{CoO,CoN}}^*(dxz)$
3 ¹ A	555.36	0.0001	-0.1003	0.1181	1.7963	121.5	$dxy(p\pi) + n_O \rightarrow \sigma_{\text{CoO,CoN}}^*(dx^2-y^2)$
4 ¹ A	524.00	0.0042	-0.0122	0.6840	1.7630	90.4	$dz^2(p\sigma) + n_O \rightarrow \sigma_{\text{CoO,CoN}}^*(dxz)$
5 ¹ A	408.59	0.0002	-0.0078	0.1249	0.1074	124.6	$dyz(p\sigma) + n_O \rightarrow \sigma_{\text{CoO,CoN}}^*(dxz)$
6 ¹ A	391.24	0.0004	-0.0175	0.1708	0.1588	127.0	$dxy(p\pi) + n_O \rightarrow \sigma_{\text{CoO,CoN}}^*(dx^2-y^2)$
7 ¹ A	381.55	0.0012	0.0614	0.3094	0.1984	14.7	$dz^2(p\sigma) + n_O \rightarrow \sigma_{\text{CoO,CoN}}^*(dx^2-y^2)$
$C_{2v}(SS,RR)(\lambda)(\delta'\delta')_e(\lambda\lambda)_a[\text{Co(DMEDDS)}]^-$							
1 ¹ B	576.33	0.0007	0.0792	0.2969	1.6879	80.7	$dyz(p\sigma) + n_O \rightarrow \sigma_{\text{CoO,CoN}}^*(dx^2-y^2)$
2 ¹ A	558.16	0.0000	-0.0458	0.0328	1.8138	180.0	$dxy(p\pi) + n_O \rightarrow \sigma_{\text{CoO,CoN}}^*(dx^2-y^2)$
2 ¹ B	533.74	0.0036	-0.0503	0.6417	1.7759	92.4	$dz^2(p\sigma) + n_O \rightarrow \sigma_{\text{CoO,CoN}}^*(dxz)$
3 ¹ A	410.16	0.0002	-0.0096	0.1172	0.0818	180.0	$dyz(p\sigma) + n_O \rightarrow \sigma_{\text{CoO,CoN}}^*(dxz)$
3 ¹ B	394.77	0.0003	-0.0201	0.1577	0.1520	141.3	$dxy(p\pi) + n_O \rightarrow \sigma_{\text{CoO,CoN}}^*(dxz)$
4 ¹ A	383.36	0.0011	0.0535	0.2971	0.1732	0.0	$dz^2(p\sigma) + n_O \rightarrow \sigma_{\text{CoO,CoN}}^*(dx^2-y^2)$

[†] $dyz(p\sigma) = dyz + \sigma_{\text{COO}}$; $dz^2(p\sigma) = dz^2 + \sigma_{\text{CoO,CoN}}$. See footnotes of Tables 2 and 3 for other information.

form of the *B*-ring much like a five-membered ring. In this way, the absolute configurations can be clearly specified by combining the chirality notations, as depicted in Figure 2, where the notations are grouped in the sequence: symmetry, Δ/Λ for the octahedral core, (*R/S*) for chiral carbons and/or nitrogens with the former first, (δ/λ) for the backbone *E*-ring, and ($\delta/\lambda \dots \delta/\lambda$) for other chelate rings. In addition, the subscript *e/a* means equatorial/axial, and the prime (') is used to indicate six-membered rings for clarity.

Initial geometries of the chelates *cis-eq*-[Co(ED3A-type)(*X*)]⁻ (*X* = CN⁻, NO₂⁻) and *trans*-(O₅)-[Co(EDDS-type)]⁻ were constructed by referring to the X-ray structures [Co(ED3A)(CN)]⁻ [11], [Co(ED3A)(NO₂)]⁻ [22], and [Co(EDDS)]⁻ [23–25]. The ground-state geometry optimizations and subsequent frequency calculations were performed employing the DFT method with tight convergence criterion and ultrafine integral grid, as implemented in the Gaussian09 program package [26]. Different functionals have been tested, and finally the B3P86 [27, 28] and B3LYP [27, 29, 30] hybrid functionals together with the 6-311++G(2d,p) basis

set were used in the calculations of ED3A-type and ED3A-type complexes, respectively. The excitation energies, oscillator and rotational strengths of the 30 lowest-lying singlet excited states for the optimized geometries were then calculated using the TDDFT method with the same functional and basis set. In all cases, solvent (water) effects have been included using the polarizable continuum model [31] (PCM) in the integral equation formalism (IEF).

3. Results and Discussions

3.1. Optimized Geometry Parameters

The optimized geometries for the ground states of the two series of chelates have been verified by frequency calculations without imaginary frequencies. Two typical structures are pictorially given in Figures 2c and d, the others can be found in the supporting materials (available upon request from the author). A brief comparison between the optimized and observed bond parameters for *cis-eq*-C₁A(*R*)(δ)($\lambda\lambda\lambda$)[Co(ED3A)(NO₂)]⁻ and *trans*-

Table 5. Calculated *N*-vicinal effects on the first three *d*-*d* transitions of the two series chelates *cis*-*eq*-[Co(ED3A-type)(X)]⁻ (*X* = CN⁻, NO₂⁻) and *trans*-(O₅)-[Co(EDDS-type)]⁻.

Excited States	Rotational Strengths (DBM)			<i>N</i> -Vicinal effects (DBM)				
	Unsub ^a	Optim ^b	Fixed ^c	Total	Substituent	% ^d	Relaxation	% ^d
(a) C ₁ A(<i>R</i>)(δ)($\lambda\lambda\lambda$)[Co(MED3A)(CN)] ⁻								
2 ¹ A	-0.0240	0.0149	0.0220	-0.0389	-0.0459	118	0.0070	-18
3 ¹ A	0.0047	-0.0052	-0.0090	0.0099	0.0137	138	-0.0038	-38
4 ¹ A	0.0497	-0.0059	0.0021	0.0555	0.0476	86	0.0079	14
(b) C ₁ A(<i>R</i>)(δ)($\lambda\lambda\lambda$)[Co(MED3A)(NO ₂)] ⁻								
2 ¹ A	-0.0202	0.0355	0.0452	-0.0556	-0.0654	118	0.0097	-18
3 ¹ A	-0.0423	0.0027	-0.0525	-0.0450	0.0102	-23	-0.0552	123
4 ¹ A	0.0772	-0.0380	0.0303	0.1152	0.0469	41	0.0683	59
(c) C ₁ A(<i>R</i>)(δ)($\lambda\lambda\lambda$)[Co(BED3A)(NO ₂)] ⁻								
2 ¹ A	-0.0202	0.0479	0.0683	-0.0681	-0.0885	130	0.0204	-30
3 ¹ A	-0.0423	-0.0557	-0.0515	0.0134	0.0092	69	0.0042	31
4 ¹ A	0.0772	-0.0123	-0.0054	0.0895	0.0826	92	0.0070	8
(d) C ₁ A(<i>SS,RR</i>)(λ)($\delta'\delta'$) _a ($\lambda\lambda$)[Co(MEDDS)] ⁻								
2 ¹ A	0.0949	0.0917	0.1435	0.0032	-0.0486	-1544	0.0518	1644
3 ¹ A	-0.1299	-0.1003	-0.1495	-0.0296	0.0195	-66	-0.0492	166
4 ¹ A	0.0332	-0.0122	-0.0130	0.0454	0.0461	102	-0.0007	-2
(e) C ₂ A(<i>SS,RR</i>)(λ)($\delta'\delta'$) _e ($\lambda\lambda$) _a [Co(DMEDDS)] ⁻								
1 ¹ B	0.0949	0.0792	0.2071	0.0157	-0.1122	-714	0.1279	814
2 ¹ A	-0.1299	-0.0458	-0.1793	-0.0841	0.0494	-59	-0.1335	159
2 ¹ B	0.0332	-0.0503	-0.0650	0.0835	0.0982	118	-0.0147	-18

^a Rotational strengths of the unsubstituted chelates: [Co(ED3A)(CN)]⁻ for (a), [Co(ED3A)(NO₂)]⁻ for (b) and (c), and [Co(EDDS)]⁻ for (d) and (e). ^b Rotational strengths for optimized geometries of the chelates (a)–(e). ^c Rotational strengths for fixed geometries constructed from the unsubstituted chelates by replacing the hydrogen atoms on asymmetric nitrogens with the methyl (M) or benzyl (B) groups without geometry re-optimization. ^d Percentage of substituent/relaxation effects to the total vicinal effects.

(O₅)-C₂A(*SS,RR*)(λ)($\delta'\delta'$)_e($\lambda\lambda$)_a[Co(EDDS)]⁻ isomers is listed in Table 1.

For the chelate *cis*-*eq*-[Co(ED3A)(NO₂)]⁻, the agreement between calculated and observed values is very good, except for the dihedral angle N1–Co–N3–O8. This exception in dihedral angle means that the calculated orientation of the nitro plane relative to the Co–N1 bond in water solution is quite different from that in crystal, because we did not find another stable isomer with a different nitro orientation. However, for its *N*-methyl-substituted chelate *cis*-*eq*-[Co(MED3A)(NO₂)]⁻, we got two stable conformers with the relative energy difference of 1.50 kcal/mol including the zero-point energy (ZPE) correction, which are structurally different only in the nitro orientation. The dihedral angle N1–Co–N3–O8 for the lowest energy conformer (conformer **1**) is -40.5°, while for the higher energy conformer (conformer **2**), it is 54.3°. Similarly, for the *N*-benzyl-substituted ED3A chelate *cis*-*eq*-[Co(BED3A)(NO₂)]⁻, the dihedral angles of the corresponding conformers are -40.6° and 57.3°, respectively, with the relative energy of 1.67 kcal/mol.

The influence of different orientations of the nitro plane on the ECD spectra will be discussed later.

For the chelate *trans*-(O₅)-[Co(EDDS)]⁻, however, the agreement between calculated and measured results is not as good as that in ED3A complex. The largest deviation occurs in the bond lengths of Co–N1 and Co–O1. We have tested other functionals and found that the PBE1PBE [32, 33] functional (also called PBE0 [34]) can significantly improve the metal–ligand bond lengths, giving 1.930 Å for Co–N1 and 1.898 Å for Co–O1; but it seems systematically underestimating some C–C and N–C bond lengths, e. g., yielding 1.474 Å for N1–C7. Since the N–C bond lengths are also our main concern, for which the results based on B3LYP functional are clearly better than those of PBE1PBE, therefore the B3LYP results will be preferred.

3.2. DFT Energy Levels and Kohn–Sham Orbitals

The calculated DFT energy levels and Kohn–Sham (KS) orbitals for the two series of chelates have been

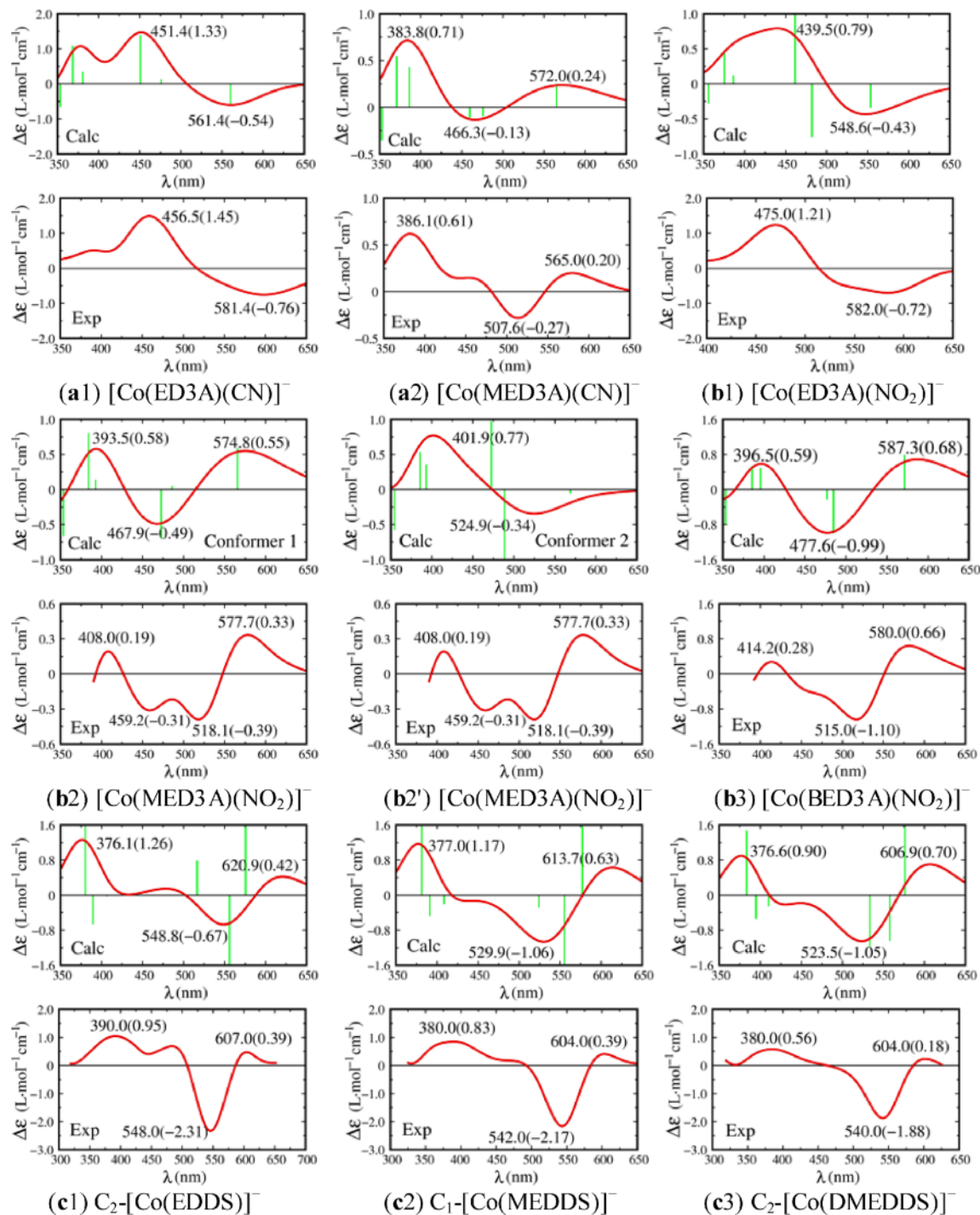


Fig. 3 (colour online). Comparison of the calculated and observed [10–12] ECD spectra: (a1) and (a2) the *cis-eq*- $\text{C}_1\Lambda(R)(\delta)(\lambda\lambda\lambda)[\text{Co}(\text{ED3A-type})(\text{CN})]^-$ series; (b1)–(b3) the *cis-eq*- $\text{C}_1\Lambda(R)(\delta)(\lambda\lambda\lambda)[\text{Co}(\text{ED3A-type})(\text{NO}_2)]^-$ series; (c1)–(c3) the *trans*- $(\text{O}_5)\text{-}\Lambda(\text{SS},\text{RR})(\lambda)(\delta'\delta')_e(\lambda\lambda)_a[\text{Co}(\text{EDDS-type})]^-$ series. Note that the two conformers (b2) and (b2') are structurally different only in the nitro orientations.

analyzed carefully in order to elucidate and assign the related transitions. To facilitate comparisons, the orientation of the coordinate system depicted in Figure 2d for the C_2 -symmetric *trans*-(O_5)-[Co(EDDS)][−] chelate has been taken as the standard orientation for other chelates. Detailed analyses of the KS orbitals revealed that, in all cases, the lowest two unoccupied orbitals are dominated by the dxz and dx^2-y^2 atomic orbitals of the central Co(III) ion, forming the typical $\sigma_{CoO,CoN}^*$ antibonding orbitals with the four (in the equatorial plane) or six (including the axial direction) coordinating atoms, respectively. In the occupied orbitals, three are dominated by the dyz , dxy , and dz^2 orbitals. The other occupied orbitals are either n_O -type orbitals occupied by the lone pair electrons of carbonyl oxygens, mixed with the σ_{CCO} bonding orbitals of the glycinate or β -alaninate rings or n_{NO_2} -type and π_{NO_2} -type orbitals of the NO_2^- group. Both groups also have significant $d-p\sigma$ bonding and $d-p\pi$ conjugate characteristics due to the participation of some d orbitals. Since the general characteristics are very close to those of the [Co(EDDA-type)(L)][−] complexes [18], they will not be discussed in details here.

3.3. Rotational Strengths and Transition Moments

The calculated transition wavelengths, oscillator and rotational strengths (both in length and velocity forms), as well as the electric and magnetic transition dipole moments of the two series of chelates have been compiled in the supporting information. As the rotational strengths calculated in velocity form are independent of the choice of origin, only this form will be addressed below, though no obvious discrepancy between the two forms was observed. To facilitate discussions, the parts of results for the first six excitations of the most stable conformers, which cover the most important spectral range of $\lambda > 350$ nm, are given in Tables 2–4. To clarify the main features of the excitations, a detailed analysis in terms of chromophore transitions has been carried out, and the dominant contributions are listed in the last column of these tables.

For these chelates, the first three excitations are dominated by the typical metal-centered $d-d$ transitions with large magnetic dipole transition moments of 1.6–1.8 Bohr magneton, while the latter three are more like the weak ligand centered $n/\pi-\sigma^*$ transitions. These characteristics are quite similar to those of the [Co(EDDA-type)(L)][−] complexes [18]. However,

we noted that transitions arising from the dz^2 -orbital usually have the largest electric dipole transition moments, which are distinctly different from those of the EDDA-type complexes.

In Tables 2 and 3, the signs of rotational strengths for the first three transitions of the N -alkyl-substituted isomers are generally different from those of the corresponding unsubstituted one, indicating unambiguously the unusual vicinal effects of the ED3A-type chelates. In Table 4, the calculated rotational strengths of the first two transitions slightly decrease in magnitude with increase in the methyl substituents. This is in good agreement with the observed [12] ECD intensities of the EDDS-type complexes, and demonstrates the negligible vicinal effects.

3.4. Calculated and Observed ECD Spectra

By use of the excitation energies and rotational strengths calculated at the TDDFT level, theoretical ECD spectra for these complexes were generated as a sum of Gaussians, centered at the calculated wavelengths λ_{calc} with integral intensities proportional to the rotational strengths R of the corresponding transitions. The half bandwidths Γ at the $\Delta\varepsilon_{max}/e$ of Gaussians, were assumed as [35] $\Gamma = k\lambda_{calc}^{3/2}$ with $k = 4.234 \cdot 10^{-3}$ to best reproduce the experimental spectra (except for the series of chelates [Co(ED3A-type)(NO_2)][−], where $k = 5.773 \cdot 10^{-3}$, allowing for the influence of NO_2^-). The resulting ECD curves together with the observed [10–12] ones are displayed in Figure 3, where the green (light gray) bars indicate the calculated wavelengths and rotational strengths of the transitions. Numbers beside the ECD curves are λ_{max} and $\Delta\varepsilon_{max}$ (in parentheses) of the related absorption bands, respectively.

Generally speaking, the calculated ECD curves are in good agreement with the observed ones, except for those of [Co(MED3A)(NO_2)][−]. In the experimental ECD of this chelate, the negative band around 490 nm significantly splits into two bands, while in the calculated ECD spectrum of the most stable conformer (**b2**) the corresponding ECD band does not split. Since the conformer (**b2'**) is about 1.50 kcal/mol higher in energy than (**b2**), it seems also impossible to reproduce the experimental ECD by Boltzmann weighted average. To solve this discrepancy, we have made additional calculations, including a *trans-eq*-isomer effect, a hydrolysis effect, or the formation of a hydrogen

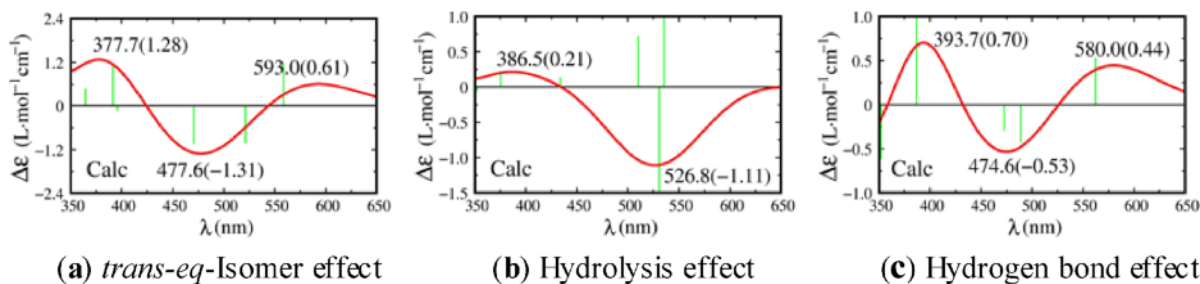


Fig. 4 (colour online). Factors which may affect the ECD curve of the *cis-eq*-[Co(MED3A)(NO₂)]⁻ isomer.

bond in solution, as depicted in Figure 4, but none of these curves look more reasonable. In view of the complicated interactions between the nitro-chelate and solvent in solution, we thought that a molecular dynamics simulation for the solvent effects may be needed to interpret the splitting of the observed band, which is beyond the scope of this paper, and will be reported later.

3.5. The Unusual *N*-Vicinal Effects

According to the interpretation of Maricondi and Douglas [9], the vicinal effect of an asymmetric nitrogen atom arises from the increase in symmetry of its

chemical environment. This means it may significantly reduce the intensity of ECD spectra but cannot reverse their sign. In such a sense, the phenomena observed in [Co(ED3A-type)(X)]⁻ and [Co(EDDS-type)]⁻ complexes could be called unusual vicinal effects.

Structurally speaking, the *N*-vicinal effects incorporate both changes in substituents and in conformations. The contribution of each change to the overall *N*-vicinal effects cannot be determined experimentally, but it could be calculated theoretically by replacing the hydrogen atom on the asymmetric nitrogen with a methyl or benzyl group and then calculating the rotational strengths or the ECD spectrum of this complex without geometry re-optimization. To reduce ar-

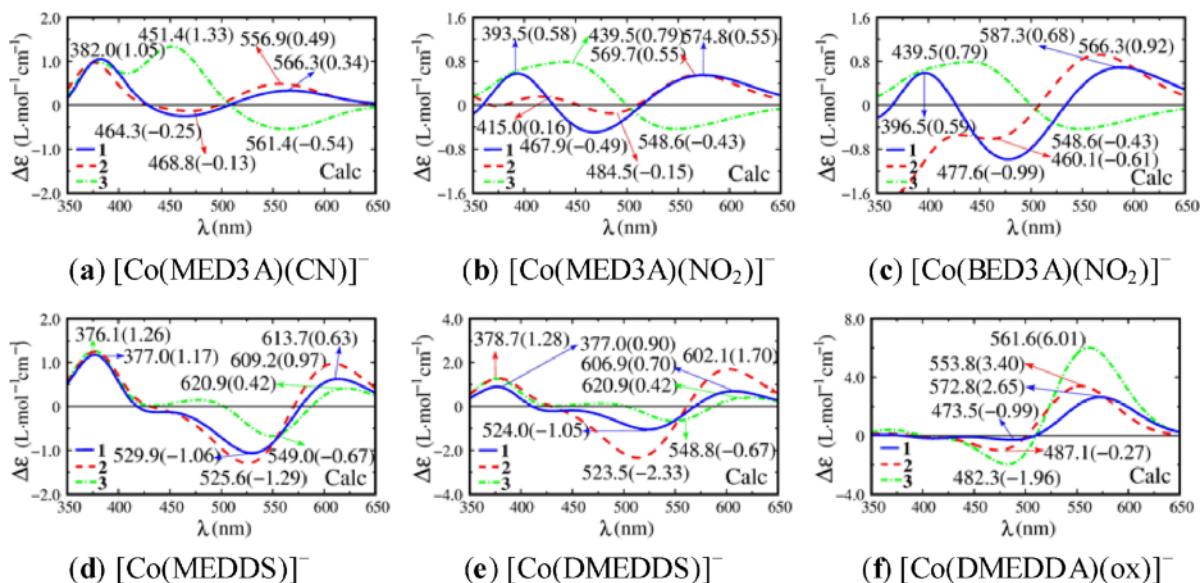


Fig. 5 (colour online). Calculated ECD curves to show the unusual and usual *N*-vicinal effects as well as the substituent effects: (a)–(c) are the typical unusual cases; (d) and (e) are less unusual; (f) is the usual or normal case. The solid blue line 1 and the dashed red line 2 are for the optimized and un-optimized geometries of the chelates, respectively, while the dash-dotted green line 3 is for the corresponding unsubstituted chelate.

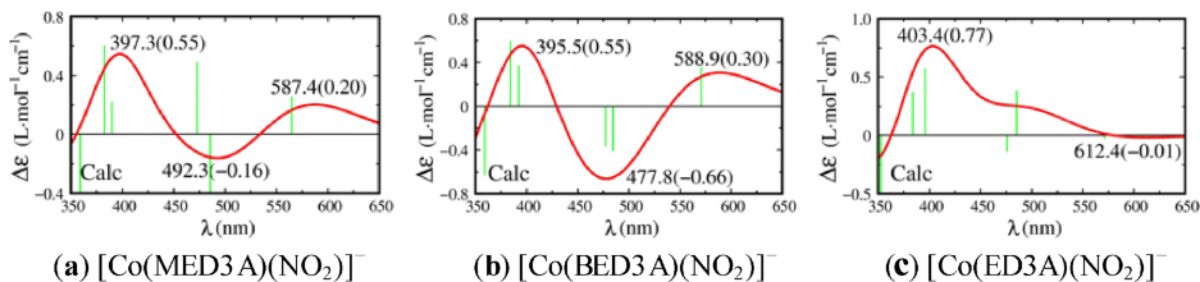


Fig. 6 (colour online). ECD curves (a) and (b) were calculated by rotating the nitro group of the *N*-alkyl-substituted chelates to the same orientation as in the unsubstituted one, and (c) was obtained by simply replacing the methyl group of $[\text{Co}(\text{MED3A})(\text{NO}_2)]^-$ by a hydrogen atom.

tificial error, the related C–N bond length and orientation of the substituent group can be determined by referring to the fully optimized geometry of this structure. Such results should contain only the contribution of the change in substituent. To facilitate comparisons, the ECD curves calculated for these ‘fixed’ geometries together with those for the fully optimized structures are shown in Figure 5, as depicted in dashed red and solid blue lines, respectively. The dash-dotted green lines are the ECD curves of the corresponding unsubstituted chelates.

This figure clearly shows the three cases of the *N*-vicinal effects: (a)–(c) are the typical unusual cases calculated for the $[\text{Co}(\text{ED3A-type})(\text{X})]^-$ complexes, in which the *N*-vicinal effects reverse the sign of the ECD curve of $[\text{Co}(\text{ED3A})(\text{CN})]^-$, (d) and (e) are the less unusual cases calculated for the $[\text{Co}(\text{EDDS-type})]^-$ chelates, in which the *N*-vicinal effects are negligible; (f) is the usual or normal case calculated for the $[\text{Co}(\text{EDDA-type})(\text{ox})]^-$ chelate [18], where the *N*-vicinal effects sharply decrease the ECD intensity of the $[\text{Co}(\text{EDDA})(\text{ox})]^-$ chelate. It can be seen from the figure that nearly in all cases the red curves are close or

very close to the blue lines. This means the change in substituents, or the substituent effect, makes dominant contribution to the total *N*-vicinal effects.

For the nitro-chelates $[\text{Co}(\text{MED3A})(\text{NO}_2)]^-$ and $[\text{Co}(\text{BED3A})(\text{NO}_2)]^-$, the small difference between the two curves in the long wavelength region may also indicate that the possible effects resulting from the preferred orientation of the coordinated nitro group are small. To confirm this conjecture, we calculated their ECD curves using their optimized geometries modified by rotating the nitro group to the same orientation as in the unsubstituted one (i. e., the dihedral angle N1–Co–N3–O8 is 28.0°) or replacing the methyl group by a hydrogen atom without geometry re-optimizations. The results are shown in Figure 6. Since the curves in Figures 6a and b are very similar to the blue (solid) lines in Figures 5b and c, respectively, it is evident that the reorientation or at least the rigid rotation of the nitro group makes little contribution to the unusual vicinal effects. Figure 6c represents the contribution of the geometry change from $[\text{Co}(\text{ED3A})(\text{NO}_2)]^-$ to $[\text{Co}(\text{MED3A})(\text{NO}_2)]^-$ with no substituent effects, which accounts for the bigger difference between the

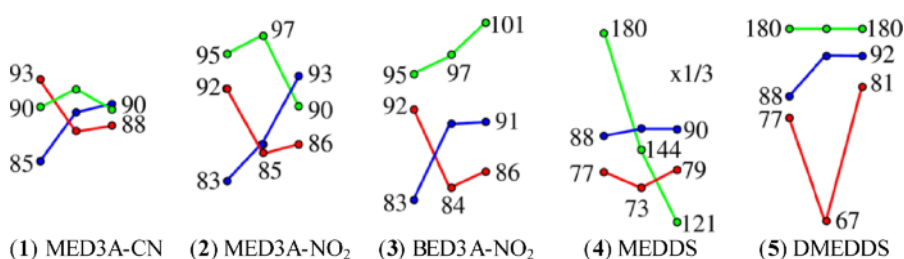


Fig. 7 (colour online). Variations of the angle (θ) between the electric (μ) and magnetic (m) dipole transition moments with the geometries of the chelates: unsubstituted (the start points of the lines), substituted without (middle points), substituted with (last points) geometry optimization. The first three transitions are represented by red (gray), green (light gray), and blue (dark) lines, respectively. Angles are in degrees.

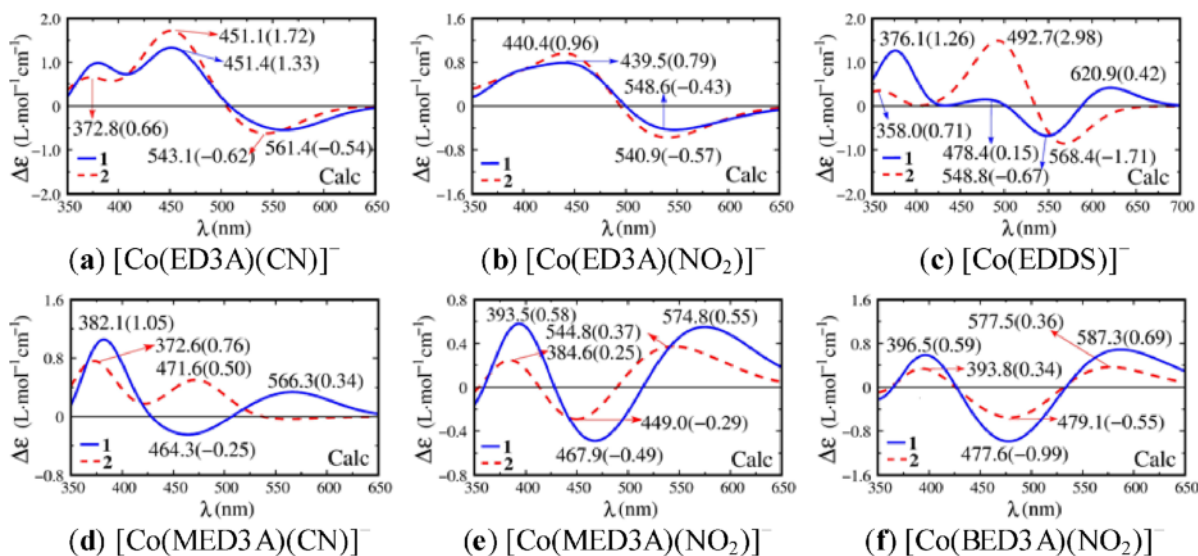


Fig. 8 (colour online). Calculated CD curves of the chelates (a) [Co(ED3A)(CN)]⁻, (b) [Co(ED3A)(NO₂)]⁻, (c) [Co(EDDS)]⁻, and the *N*-alkyl-substituted ED3A-type complexes (d)–(f), with (solid blue line 1) or without (dashed red line 2) the contributions of the octahedral core.

red (dashed) and blue (solid) curves in the short wavelength region of Figures 5b and c. In addition, for the two conformers of [Co(MED3A)(NO₂)]⁻ we also found that the big difference between their ECD curves (Figs. 3b2, b2') is not dominated by the nitro reorientation, but by the dihedral angle N1–C1–C2–N2 of the *E*-ring: It is 54.0° for conformer 1, and 51.7° for conformer 2.

Experimentally, the *N*-vicinal effects were measured [9, 10] by subtracting the ECD curve of the *N*-alkyl-substituted chelate from that of the unsubstituted one. Theoretically, it is not only convenient but also necessary to calculate the vicinal effects as differences in rotational strengths instead of the ECD curves, because exact band-shape functions for the transitions are not available. The generally used Gauss line-shape functions and assumed half band widths may yield incorrect conclusions in some cases. For this reason, the *N*-vicinal effects of the chelates have been calculated by subtracting the rotational strengths of the fully-optimized geometries (3rd column in Table 5) from those of corresponding unsubstituted chelates (2nd column). The results for the first three *d*–*d* transitions are shown in the 5th column in Table 5. Similarly, contributions of the change in substituents to the total *N*-vicinal effects were obtained by subtracting the rotational strengths of the fixed geometries (4th column)

from those of the unsubstituted chelates and have been given in the 6th column, followed by its percentage to the total vicinal effects. As differences between the total vicinal effects and the substituent effects, the contributions of change in conformations can be found in the 8th column. As seen from this table, the substituent effects are usually the dominant components of the *N*-vicinal effects, while the conformational relaxation effects are in most cases opposite in sign to the substituent effects for the first two transitions. Therefore, the total *N*-vicinal effects are the partially cancelled results of the two contributions.

3.6. The Origin of Unusual *N*-Vicinal Effects

Previously, we have discussed the structural factors responsible for the *N*-vicinal effects. In the view of electron transitions, however, these structural factors must play a role to alter the rotational strengths of transitions. To check how they are functioning, the angles (θ) between the electric (μ) and magnetic (m) dipole transition moments as a function of the structures of unsubstituted, substituted without and with geometry optimization, have been plotted in Figure 7. In which, the first three transitions are represented by the red (gray), green (light gray), and blue (dark) lines, respectively. What we see immediately from this figure is

that: For the first three transitions of the $[\text{Co}(\text{ED3A-type})(\text{X})]^-$ chelates, the angle θ varies not very much but always around 90° ; especially in the first and third transitions, it always passes through the 90° in the variation of the chelate structure, which leads to the change in sign of the rotational strengths. This phenomenon has not been observed in the $[\text{Co}(\text{EDDS-type})]^-$ series chelates as well as in others we have treated.

We thought that this phenomenon might be associated with the chirality of the octahedral core $\text{CoN}_3\text{O}_3/\text{CoN}_2\text{O}_3\text{C}$, because the octahedral core of the *cis-eq*- $[\text{Co}(\text{ED3A})(\text{X})]^-$ isomer has no net chirality according to the IUPAC rules [20] or ring-pairing method [21], as has been mentioned in the section of computational details. We could assign it a Λ -chirality, of course, according to the distribution of the chelate rings around the pseudo- C_3 -symmetry axis, but remember that only two of the four chelate rings make contributions to this chirality. It means that the Λ -type octahedral core may make less contribution to the optical activities of these series chelates. To confirm this guess, we propose a novel method to calculate the ECD curves of the chelates, namely, without contribution of the octahedral core. The first step is performing a restricted geometry optimization for the chelates by confining the octahedral core with a C_s -symmetry. The second step is the conventional TDDFT calculation using the geometries obtained in the first step. Since the octahedral core now has mirror symmetry, it cannot make direct contributions to the optical activity of the chelates. In this way, we have calculated the ECD spectra of all the chelates mentioned above. Parts of them are displayed in Figure 8.

As expected, the minor difference between the ECD curves depicted in Figures 8a or b clearly show that the contribution of the octahedral core to the optical activity of the ED3A chelates is very small; while in the EDDS chelate (Fig. 8c), it makes a significant contribution. Compared with the unsubstituted ED3A chelates, Figures 8d–f indicate that the contribution of the octahedral core in the *N*-alkyl-substituted ED3A-type complexes increases in certain degree. Although the increase is not very much, the results are significant: For the chelate $[\text{Co}(\text{MED3A})(\text{CN})]^-$, it is this increase that reverses the sign of the first two ECD bands, because the dashed red curve is quite different from the solid blue one; for chelates $[\text{Co}(\text{MED3A})(\text{NO}_2)]^-$ and $[\text{Co}(\text{BED3A})(\text{NO}_2)]^-$, this increase is also a major factor to change the sign of the first two bands, albeit

it is not the unique factor due to the red curves being already similar to the blue ones in shape (but not in intensity). Note that for most cobalt(III) chelates with a Λ -type octahedral core, the first ECD band is positive and the second one negative. Therefore, the ECD spectra of the unsubstituted chelates $[\text{Co}(\text{ED3A})(\text{X})]^-$ are special since their first two ECD bands have opposite sign to the normal cases. In other words, the unusual vicinal effects observed in this series chelates reflects an increase in the contribution of the octahedral core or a recovery in the sign of the ECD spectra from the special cases (unsubstituted) to the normal ones (substituted).

Besides this, Figure 8 also supplies some information on the equilibrium structure of the ED3A chelate in solution, because the curve shape of the dashed red line in Figure 8a looks slightly similar to the experimental spectrum than that of the blue line. This fact may tell us that the octahedral core makes no contribution to the experimental ECD due to thermal vibrations of the chelate, but it makes some contribution, though very small, to the lowest energy conformer.

At this stage, we see that the unusual *N*-vicinal effects of the cobalt(III) ED3A-type complexes originate from the negligible chirality of the octahedral core in the unsubstituted ED3A chelates. For this reason, the optical activity of the ED3A chelates is dominated by the asymmetric nitrogens and the *E*-ring conformations. It might be hard, if not impossible, to separate the two contributions, because the asymmetric nitrogens act as bridge atoms between the octahedral core and the *E*-ring. Any change on these atoms will lead to significant change in the chiroptical properties of the ED3A chelates.

4. Conclusions

In this paper, we have presented a detailed theoretical analysis for the unusual *N*-vicinal effects on the electronic circular dichroism spectra of the cobalt(III) complexes with ED3A-type and EDDS-type ligands at the DFT/B3P86/6-311++G(2d,p) level of theory (for EDDS-type complexes, the functional is B3LYP). The optimized geometries and calculated ECD curves of the chelates are in good agreement with the observed ones. Based on this agreement, the characteristics of the usual, less usual, and unusual *N*-vicinal effects as well as related chiral stereochemistry phenomena have been discussed. To reveal the origin of the unusual *N*-

vicinal effects, a novel calculation scheme has been proposed, which permits efficiently assessing the contribution of the octahedral core to the optical activity of the chelates. The main conclusions are as follows:

The vicinal effects of asymmetric nitrogens incorporate both the substituent effects and conformational relaxation effects. They usually make opposite contributions to the overall *N*-vicinal effects for the first two *d*–*d* transitions of the cobalt(III) ED3A-type and EDDS-type chelates, with the former being dominant.

The unusual *N*-vicinal effects observed in the cobalt(III) ED3A-type chelates originate from the negligible chirality of the octahedral core in the unsubstituted complexes. For this reason, the optical activity of the ED3A chelates is dominated by the asymmetric nitrogens. Any change on these atoms will lead to a significant change in the chiroptical properties. The unusual vicinal effects reflect an increase in the chi-

rality of the octahedral core, which recover the ECD spectra from the special cases to the normal ones.

These findings provide some insight into the unusual *N*-vicinal effects as well as the chiroptical properties of the chelates.

Acknowledgement

We gratefully acknowledge the financial support from the National Natural Science Foundation of China (Grant No. 21273139).

Supporting Information

The optimized geometries including Cartesian coordinates, DFT energy levels, selected Kohn–Sham orbitals, as well as the excitation energies, oscillator and rotational strengths of the dominant transitions are available upon request from the author.

- [1] C. J. Hawkins, *Absolute Configuration of Metal Complexes*, Wiley-Interscience, New York 1971.
- [2] Y. Saito, *Coord. Chem. Rev.* **13**, 305 (1974).
- [3] F. E. Jorge, J. Autschbach, and T. Ziegler, *Inorg. Chem.* **42**, 8902 (2003).
- [4] F. E. Jorge, J. Autschbach, and T. Ziegler, *J. Am. Chem. Soc.* **127**, 975 (2005).
- [5] F. S. Richardson, *The Optical Activity of Lanthanide and Transition Metal Complexes*, (Ed. S. F. Mason), in: *Optical Activity and Chiral Discrimination*, D. Reidel Pub. Comp., Dordrecht 1979, pp 107–160.
- [6] R. Kuroda and Y. Saito, *Circular Dichroism of Inorganic Complexes: Interpretation and Application*, (Eds. K. Nakanishi et al.), in: *Circular Dichroism Principles and Applications*, VCH, New York 1994, pp 217–258.
- [7] S. F. Mason, *J. Chem. Soc. A*, 667 (1971).
- [8] F. S. Richardson, *Inorg. Chem.* **11**, 2366 (1972).
- [9] C. W. Maricondi and B. E. Douglas, *Inorg. Chem.* **11**, 688 (1972).
- [10] C. W. Maricondi and C. Maricondi, *Inorg. Chem.* **12**, 1524 (1973).
- [11] D. J. Radanovic, S. R. Trifunovic, D. E. Bause, C. Maricondi, J. E. Abola, and B. E. Douglas, *Inorg. Chem.* **26**, 3994 (1987).
- [12] W. T. Jordan and J. I. Legg, *Inorg. Chem.* **13**, 2271 (1974).
- [13] A. G. Karipides and T. S. Piper, *J. Chem. Phys.* **40**, 674 (1964).
- [14] T. S. Piper and A. G. Karipides, *Inorg. Chem.* **4**, 923 (1965).
- [15] B. Bosnich and J. MacB. Harrowfield, *J. Am. Chem. Soc.* **94**, 3425 (1972).
- [16] M. A. L. Marques, C. A. Ullrich, F. Nogueira, A. Rubio, K. Burke, and E. K. U. Gross (Eds.), *Time-Dependent Density Functional Theory*, Springer, Berlin, Heidelberg 2006.
- [17] Y. Wang, Y. Wang, J. Wang, Y. Liu, and Y. Yang, *J. Am. Chem. Soc.* **131**, 8839 (2009).
- [18] A. Wang, Y. Wang, J. Jia, L. Feng, C. Zhang, and L. Liu, *J. Phys. Chem. A* **117**, 5061 (2013).
- [19] D. Radanovic, *Coord. Chem. Rev.* **54**, 159 (1984).
- [20] N. G. Connelly, T. Damhus, R. M. Hartshorn, and A. T. Hutton (Eds.), *The Red Book – Nomenclature of Inorganic Chemistry: IUPAC Recommendations*, RSC Pub., London 2005.
- [21] J. I. Legg and B. E. Douglas, *J. Am. Chem. Soc.* **88**, 2697 (1966).
- [22] J. D. Bell and G. L. Blackmer, *Inorg. Chem.* **12**, 836 (1973).
- [23] F. Pavelcik and J. Majer, *Acta Cryst.* **34**, 3582 (1978).
- [24] E. Horn, M. R. Snow, and E. R. T. Tiekink, *Z. Kristallogr.* **205**, 140 (1993).
- [25] R. E. Marsh, *Acta Cryst.* **58**, 893 (2002).
- [26] M. J. Frisch, G. W. Trucks, H. B. Schlegel, G. E. Scuseria, M. A. Robb, J. R. Cheeseman, G. Scalmani, V. Barone, B. Mennucci, G. A. Petersson, H. Nakatsuji, M. Caricato, X. Li, H. P. Hratchian, A. F. Izmaylov, J. Bloino, G. Zheng, J. L. Sonnenberg, M. Hada, M. Ehara, K. Toyota, R. Fukuda, J. Hasegawa, M. Ishida, T. Nakajima, Y. Honda, O. Kitao, H. Nakai,

- T. Vreven, Jr. J. A. Montgomery, J. E. Peralta, F. Ogliaro, M. Bearpark, J. J. Heyd, E. Brothers, K. N. Kudin, V. N. Staroverov, R. Kobayashi, J. Normand, K. Raghavachari, A. Rendell, J. C. Burant, S. S. Iyengar, J. Tomasi, M. Cossi, N. Rega, J. M. Millam, M. Klene, J. E. Knox, J. B. Cross, V. Bakken, C. Adamo, J. Jaramillo, R. Gomperts, R. E. Stratmann, O. Yazyev, A. J. Austin, R. Cammi, C. Pomelli, J. W. Ochterski, R. L. Artin, K. Morokuma, V. G. Zakrzewski, G. A. Voth, P. Salvador, J. J. Dannenberg, S. Dapprich, A. D. Daniels, O. Farkas, J. B. Foresman, J. V. Ortiz, J. Cioslowski, D. J. Fox, Gaussian 09, Revision A.02, Gaussian, Inc., Wallingford CT, 2009.
- [27] A. D. Becke, *J. Chem. Phys.* **98**, 5648 (1993).
- [28] J. P. Perdew, *Phys. Rev. B* **33**, 8822 (1986).
- [29] C. Lee, W. Yang, and R. G. Parr, *Phys. Rev. B* **37**, 785 (1988).
- [30] B. Miehlich, A. Savin, H. Stoll, and H. Preuss, *Chem. Phys. Lett.* **157**, 200 (1989).
- [31] J. Tomasi, B. Mennucci, and R. Cammi, *Chem. Rev.* **105**, 2999 (2005).
- [32] J. P. Perdew, K. Burke, and M. Ernzerhof, *Phys. Rev. Lett.* **77**, 3865 (1996).
- [33] J. P. Perdew, K. Burke, and M. Ernzerhof, *Phys. Rev. Lett.* **78**, 1396 (1997).
- [34] C. Adamo and V. Barone, *J. Chem. Phys.* **110**, 6158 (1999).
- [35] A. Brown, C. M. Kemp, and S. F. Mason, *J. Chem. Soc. A*, 751 (1971).